SIAM J. Imaging Sciences
Vol. 10, No. 4, pp. 2119–2139

A Factorization Method for Multifrequency Inverse Source Problems with Sparse Far Field Measurements*

Roland Griesmaier† and Christian Schmiedecke†

Abstract. We consider a multifrequency inverse source problem for time-harmonic acoustic or electromagnetic waves with a limited set of far field data. Assuming that far field measurements of the wave radiated by a collection of compactly supported sources are available across a whole frequency band but only at a few observation directions, we develop a noniterative reconstruction scheme of factorization type to locate the support of the sources. The method produces a union of convex polygons with normals in the observation directions that approximate the positions and the geometry of well-separated source components. The only requirement is that the unknown sources satisfy a certain coercivity assumption. Perhaps the most significant point is that the reconstruction algorithm efficiently utilizes the multifrequency information contained in the given data such that already a very small number of observation directions is sufficient to obtain a good impression about the location of the sources. We provide a rigorous justification of the reconstruction algorithm and present numerical results that illustrate our theoretical findings. A possible extension of the method to the linearized inverse medium scattering problem is briefly sketched.

Key words. inverse source problem, multifrequency, factorization method

AMS subject classifications. 35R30, 65N21

DOI. 10.1137/17M111290X

1. Introduction.

In this work we present a new approach for locating an ensemble of compactly supported time-harmonic acoustic or electromagnetic sources from far field observations of the radiated wave across a whole *frequency band* $(0, k_{\max}) \subseteq \mathbb{R}$ but only at a few (finitely many) pairs of *observation directions*

$$\{\pm\theta_1, \dots, \pm\theta_J\} =: \Theta \subseteq S^{d-1},$$

where $d = 2, 3$ denotes the dimension. The aim is to develop a reconstruction method that efficiently utilizes multifrequency information in order to reduce the number of sensor locations required to obtain a useful reconstruction of the support of the sources. This is practically relevant because it is easier to vary frequency than to change the location of a sensor.

Using the Helmholtz equation as our model for time-harmonic wave propagation, the *far field data* measured for each pair of receiver directions $\pm\theta_j$ coincide up to a constant factor with the d-dimensional Fourier transform of the superposition of sources restricted to the lines

$$\{t\theta_j \mid -k_{\max} < t < k_{\max}\}, \qquad 1 \le j \le J,$$

*Received by the editors January 23, 2017; accepted for publication (in revised form) June 27, 2017; published electronically November 21, 2017.
http://www.siam.org/journals/siims/10-4/M111290.html

†Institut für Mathematik, Universität Würzburg, 97074 Würzburg, Germany (roland.griesmaier@uni-wuerzburg.de, christian.schmiedecke@mathematik.uni-wuerzburg.de).

of length $2k_{\max}$ through the origin. Hence, the inverse problem we are concerned with consists in recovering the support of a function given its Fourier transform on a subset of the Fourier domain that is band-limited and highly sparse.

Since without further assumptions neither the sources nor their support are uniquely determined by the given data, a classical approach would be to consider a least squares formulation with a suitable regularization to approximate the source with smallest L^2-norm that is compatible with the data. However, in practice it is often difficult to recover useful information on the support of a source from such regularized least squares solutions. In general no upper bounds on the support of a source can be obtained from sparse multifrequency far field data sets as considered in this work, because there exist so-called nonradiating sources with arbitrarily large support that radiate waves with vanishing far fields. However, Sylvester and Kelly [34] recently established rigorous lower bounds for the support of a source in terms of sparse multifrequency far field data sets. Their so-called Θ-convex scattering support is a single Θ-convex polygon (a convex polygon with normals in the directions $\pm\theta_j$, $j = 1, \dots, J$) that is uniquely determined by the data and must be contained in any Θ-convex polygon which contains the source.

We follow this idea but discuss a restricted setting, assuming that the real part of a complex multiple of the sources is bounded away from zero on their support. Henceforth, we call this a coercivity assumption on the sources. In the most important application that we have in mind, which is linearized inverse medium scattering, this coercivity assumption corresponds to coercivity constraints on the contrast of the index of refraction of the scatterers relative to the background medium.

We develop a factorization method [23, 25] that recovers not only a single but a union of Θ-convex polygons which approximate the well-separated components of the support of the ensemble of sources. We show that these reconstructions must be contained in the Θ-convex hull of the support of the whole collection of sources (the smallest Θ-convex polygon which contains this support) and that they must contain the Θ-convex hulls of the supports of the individual source components. We mention that our coercivity assumption implies that the Θ-convex hull of the support of a source actually coincides with the corresponding Θ-convex scattering support.

We start by considering a single pair of observation directions $\pm\theta_j$ and use the corresponding far field data to define a convolution operator F^{θ_j}. We show that this operator admits a *factorization*

$$F^{\theta_j} = L_D^{\theta_j} T_D \left(L_D^{\theta_j}\right)^*$$

of similar structure as known from the traditional factorization method for single-frequency inverse medium scattering problems with multistatic far field data [24, 25]. The ranges of $L_D^{\theta_j}$ and of the square root of a suitable combination of the real and imaginary parts of F^{θ_j} coincide. Since the latter is known from the measurement data, we can utilize this to develop a criterion to decide (based on the given far field data) for any given function whether it belongs to the range of $L_D^{\theta_j}$. Applying this test to a suitable *test function* associated with an arbitrary *test point* $z \in \mathbb{R}^d$, we can decide whether the projection of z on the one-dimensional subspace spanned by the observation directions $\pm\theta_j$ belongs to the set-valued projection of

the support of the ensemble of sources on this subspace. This can be used to determine the smallest union of strips (intersections of parallel half spaces) with normals in the observation directions $\pm\theta_j$ that contains the support of the sources.

Combining this test for all available pairs of observation directions $\pm\theta_1, \ldots, \pm\theta_J \in \Theta$ yields an algorithm that recovers a union of Θ-convex polygons (the intersections of the unions of strips obtained for each pair of observation directions $\pm\theta_j$) that is a subset of the Θ-convex hull of the support of the whole collection of sources, which contains the Θ-convex hull of the support of each source component.

The reconstruction method considered in this work is a generalization of the MUSIC reconstruction scheme recently developed in [15] for locating point sources from given discrete multifrequency far field data. This MUSIC scheme is somewhat related to the MUSIC methods considered in [27, 28] and also to multivariate generalizations of Prony's method [7, 32]. Reconstruction methods based on similar viewpoints from within the area of inverse scattering are, e.g., the multifrequency sampling methods [12, 17, 29], the time-domain sampling methods [5, 16, 18], the scattering supports discussed in [26, 33], or the back-propagation schemes [11, 13, 14, 31]. For further recent contributions to multifrequency inverse source problems we refer, e.g., to [2, 3, 8, 35], and other methods aiming for approximating the location and shape of sources using additional a priori assumptions on the geometry and physical properties of the sources can, e.g., be found in [1, 4, 9, 10, 19, 20, 21, 22].

The outline of this paper is as follows. After describing the mathematical setup of our problem in section 2, we develop and analyze the factorization method for multifrequency measurements for a single pair of observation directions $\pm\theta_j$ in section 3. In section 4 we discuss the numerical implementation of the method for a single pair of observation directions, and in section 5 we extend the reconstruction scheme and its numerical implementation for multiple observation directions. We briefly comment on possible generalizations of the reconstruction method to the linearized inverse medium scattering problem and to frequency bands $(k_{\min}, k_{\max}) \subseteq (0, \infty)$ bounded away from zero in section 6, and we conclude with some final remarks.

2. Problem formulation.

Let

$$D := \bigcup_{m=1}^{M} D_m \subseteq \mathbb{R}^d$$

be an ensemble of finitely many well-separated bounded domains in $\mathbb{R}^d$, $d = 2, 3$, i.e., $\overline{D_j} \cap \overline{D_\ell} = \emptyset$ for $j \neq \ell$, and let $f \in L^\infty(D)$ represent a compactly supported acoustic or electromagnetic source. The time-harmonic wave $u \in H^1_{\mathrm{loc}}(\mathbb{R}^d)$ radiated by f at *wave number* $k > 0$ is modeled as the unique solution to the Helmholtz equation

$$-\Delta u - k^2 u = f \qquad \text{in } \mathbb{R}^d \tag{2.1}$$

that satisfies the Sommerfeld radiation condition

$$\lim_{r\to\infty} r^{\frac{d-1}{2}} \left(\frac{\partial u}{\partial r} - \mathrm{i}ku \right) = 0\,, \qquad r = |x|\,. \tag{2.2}$$

It is well known (see, e.g., [6]) that u has the asymptotic behavior

$$u(x;k) = C_k \frac{e^{\mathrm{i}k|x|}}{|x|^{\frac{d-1}{2}}} u^\infty(\theta_x;k) + \mathcal{O}\left(|x|^{-\frac{d+1}{2}}\right), \qquad \theta_x = \frac{x}{|x|} \in S^{d-1}, \ r = |x| \to \infty,$$

where $C_k = e^{\mathrm{i}\pi/4}/\sqrt{8\pi k}$ if $d = 2$ and $C_k = k^2/(4\pi)$ if $d = 3$, and the *far field* $u^\infty(\,\cdot\,;k)$ of $u(\,\cdot\,;k)$ is given by

$$u^\infty(\theta_x;k) = \int_D e^{-\mathrm{i}k\theta_x\cdot y} f(y)\,\mathrm{d}y = \widehat{f}(k\theta_x), \qquad \theta_x \in S^{d-1}, \tag{2.3}$$

i.e., $u^\infty(\,\cdot\,;k)$ is the Fourier transform of the source evaluated on the sphere kS^{d-1}. Throughout we refer to $u^\infty(\,\cdot\,;k)$ as the far field radiated by f at wave number k.

In the following we assume that the far field is observed at only a few, say, $2J$, *observation directions*,

$$\{\pm\theta_1, \dots, \pm\theta_J\} =: \Theta \subseteq S^{d-1}, \tag{2.4}$$

but across a whole *band of wave numbers* $k \in (0, k_{\max})$ for some $k_{\max} > 0$. Since the right-hand side of (2.3) fulfills the symmetry relation

$$\widehat{f}(k\theta_x) = \widehat{f}((-k)(-\theta_x)), \qquad \theta_x \in S^{d-1}, \ k > 0,$$

the definition of the far field immediately extends to negative wave numbers by means of

$$u^\infty(\theta;-k) := u^\infty(-\theta;k), \qquad \theta \in S^{d-1}, \ k > 0. \tag{2.5}$$

Accordingly, the measured data set is equivalent to

$$\left\{u^\infty(\theta_j;k) \mid j = 1,\dots,J, \ k \in (-k_{\max}, k_{\max}) \setminus \{0\}\right\}. \tag{2.6}$$

Our aim is to deduce information on the support of the source f from these data. However, as already mentioned in the introduction, this inverse problem is not uniquely solvable without further assumptions. For instance, as has been pointed out in [34, Prop. 4], the source

$$f := \nabla_{\theta_1^\perp} \cdots \nabla_{\theta_J^\perp} v, \qquad v \in C_0^\infty(\mathbb{R}^d),$$

where $\theta_j^\perp$ is some nonzero unit vector perpendicular to the observation directions $\pm\theta_j$ for each $j = 1,\dots,J$, and $\nabla_{\theta_j^\perp}$ denotes the directional derivative along $\theta_j^\perp$, yields a radiated wave with vanishing far field on all straight lines through the origin with direction $\pm\theta_j$, $j = 1,\dots,J$, and therefore this particular source cannot be detected from the given data set (2.6). For this reason Sylvester and Kelly [34] have introduced the notion of Θ-*convex scattering support* of (restricted) far field data as in (2.6), which is a well-defined lower bound on the Θ-convex hull of the support of the source f.

To be more specific, we define the (closed) *convex hull* of a subset $\Omega \subseteq \mathbb{R}^d$ as the intersection of all (closed) *half spaces*

$$H_{s,\theta} := \{x \in \mathbb{R}^d \mid x \cdot \theta \le s\}, \qquad \theta \in S^{d-1}, \ s \in \mathbb{R},$$

which contain it, i.e.,

$$\mathrm{ch}(\Omega) := \bigcap_{\theta \in S^{d-1}} \{x \in \mathbb{R}^d \mid x \cdot \theta \le s_\Omega(\theta)\},$$

where

$$s_\Omega(\theta) := \sup_{x \in \Omega} x \cdot \theta, \qquad \theta \in S^{d-1},$$

is the *supporting function* of Ω. Accordingly the Θ-*convex hull* of Ω is given by

$$K_{s_\Omega}(\Theta) := \bigcap_{\theta \in \Theta} \{x \in \mathbb{R}^d \mid x \cdot \theta \le s_\Omega(\theta)\},$$

and similarly we write for any single pair $\pm\theta \in S^{d-1}$

$$K_{s_\Omega}(\{\pm\theta\}) := \{x \in \mathbb{R}^d \mid s_\Omega(-\theta) \le x \cdot \theta \le s_\Omega(\theta)\}, \tag{2.7}$$

which is the smallest strip (intersection of two parallel half spaces) with normals in the directions $\pm\theta$ that contains $\overline{\Omega}$.

Remark 2.1. It is important to note that for $D = \bigcup_{m=1}^M D_m$ as above typically

$$\bigcup_{m=1}^M K_{s_{D_m}}(\Theta) \subsetneq \bigcap_{j=1}^J \bigcup_{m=1}^M K_{s_{D_m}}(\{\pm\theta_j\}) \subsetneq K_{s_D}(\Theta)$$

and even

$$\bigcup_{m=1}^M \mathrm{ch}(D_m) \subsetneq \bigcap_{\theta \in S^{d-1}} \bigcup_{m=1}^M K_{s_{D_m}}(\{\pm\theta\}) \subsetneq \mathrm{ch}(D).$$

This can easily be seen, for example, when $M = 2$ and D_1 and D_2 are two disjoint balls in $\mathbb{R}^d$, as shown in Figure 1 for $d = 2$.

In contrast to [34], we will not consider the most general case, but we add some constraints on the source f that restore a certain degree of uniqueness and that will be needed to establish the theoretical justification of the factorization method in the next section. In our main result, Theorem 3.6 below, we assume that $f \in L^\infty(D)$ is such that there exist $\tau \in \mathbb{R}$ and $c_0 > 0$ such that $\mathrm{Re}(e^{\mathrm{i}\tau} f(x)) \ge c_0$ for almost every $x \in D$. The Θ-convex scattering support and the Θ-convex hull of the support D of the source coincide in this case, and we show that this set and information on the Θ-convex hulls of the supports of the individual source components $D_1, \ldots, D_M$ can be recovered from the given data (2.6).

Remark 2.2. To put our results into perspective, we briefly discuss two related but larger data sets:

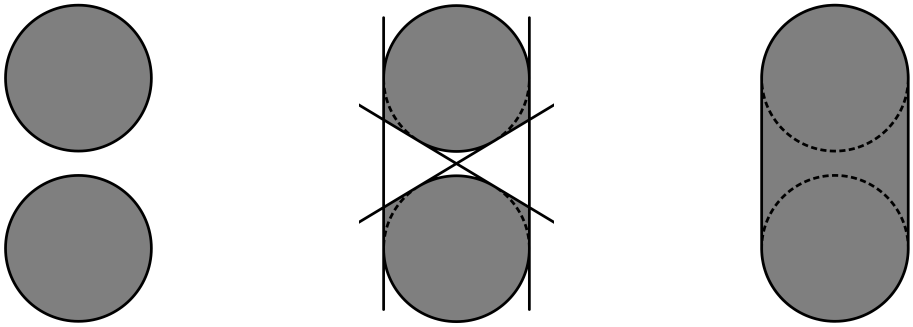

Figure 1. *Example with two disjoint disks D_1 and D_2. Left:* $\mathrm{ch}(D_1) \cup \mathrm{ch}(D_2)$ *(gray). Center:* $\bigcap_{\theta\in S^1}(K_{s_{D_1}}(\{\pm\theta\}) \cup K_{s_{D_2}}(\{\pm\theta\}))$ *(gray). Right:* $\mathrm{ch}(D_1 \cup D_2)$ *(gray).*

(a) If $u^\infty(\theta;k)$ is available for all $k \in (0,k_{\max})$ and not only for a sparse set of observation directions but for all $\theta \in S^{d-1}$, then by (2.3) this is equivalent to the knowledge of $\widehat{f}$ in the ball $B_{k_{\max}}(0)$ of radius $k_{\max}$ centered at the origin. Applying the d-dimensional inverse Fourier transform to these band-limited data directly results in a blurred reconstruction of the source. Moreover, since f is compactly supported, its Fourier transform $\widehat{f}$ is analytic and thus $\widehat{f}$ as well as the source f and its support are in fact uniquely determined by the given data. Numerically, analytic continuation is unstable of course, but the factorization method for the linearized inverse medium problem [24] can immediately be adapted to recover the support of f directly from this data set (without analytic continuation and without blurring).

(b) On the other hand, if $u^\infty(\theta;k)$ is given for the sparse set of observation directions Θ from (2.4) and not only for $k \in (0,k_{\max})$ but for all $k > 0$, then this is equivalent to the knowledge of $\widehat{f}(k\theta_j)$ for all $k \in \mathbb{R}$ and $j = 1,\dots,J$. Applying the Fourier slice theorem

$$\widehat{f}(k\theta_j) = \int_{\mathbb{R}} e^{-\mathrm{i}ks} \int_{\theta_j^\perp} f(s\theta_j+\eta)\,\mathrm{d}\eta\,\mathrm{d}s = \int_{\mathbb{R}} e^{-\mathrm{i}ks}(Rf)(\theta_j,s)\,\mathrm{d}s\,, \tag{2.8}$$

where $\theta_j^\perp$ denotes the hyperplane perpendicular to θ_j and Rf is the Radon transform of f (see, e.g., [30, Thm. 1.1]), shows that this data set is equivalent to the knowledge of $(Rf)(\theta_j,\cdot)$ for $j = 1,\dots,J$. If $f \in L^\infty(D)$ satisfies our coercivity assumption $\mathrm{Re}(e^{\mathrm{i}\tau}f(x)) \geq c_0 > 0$ for almost every $x \in D$, then clearly

$$\big\{x \in \mathbb{R}^d \,\big|\, x\cdot\theta_j \in \mathrm{supp}((Rf)(\theta_j,\cdot))\big\} = \bigcup_{m=1}^{M} K_{s_{D_m}}(\{\pm\theta_j\})\,,$$

and this set, which coincides with the smallest union of strips with normals in the directions $\pm\theta_j$ that contains $D_1,\dots,D_M$, can be approximated numerically by estimating the support of $(Rf)(\theta_j,\cdot)$. Combining these reconstructions for all observation directions yields

$$\bigcap_{j=1}^{J}\bigcup_{m=1}^{M} K_{s_{D_m}}(\{\pm\theta_j\})\,, \tag{2.9}$$

which is a subset of the Θ-convex hull $K_{s_D}(\Theta)$ of the support of f that contains the Θ-convex hull $K_{s_{D_m}}(\Theta)$ of the support D_m of each source component.

The main contribution of this article is a reconstruction algorithm that recovers the set in (2.9) from sparse band-limited data as in (2.6) (without analytic continuation and without blurring).

3. The factorization method for a single observation direction. We start by considering far field data $u^\infty(\pm\theta_j;k)$, $k\in(0,k_{\max})$, for a single pair of observation directions $\pm\theta_j$, $1\le j\le J$, and use the extension of these data to negative wave numbers in (2.5) to define the convolution operator $F^{\theta_j}:L^2(0,k_{\max})\to L^2(0,k_{\max})$,

$$\left(F^{\theta_j}\phi\right)(t) := \int_0^{k_{\max}} u^\infty(\theta_j;t-s)\phi(s)\,\mathrm{d}s\,, \qquad t\in(0,k_{\max})\,. \tag{3.1}$$

The mathematical foundation of our reconstruction method relies on a suitable factorization of F^{θ_j}. This factorization involves the operator $L_D^{\theta_j}:L^2(D)\to L^2(0,k_{\max})$,

$$\left(L_D^{\theta_j}\psi\right)(t) := \int_D e^{-\mathrm{i}t\theta_j\cdot y}\psi(y)\,\mathrm{d}y\,, \qquad t\in(0,k_{\max})\,, \tag{3.2}$$

and its adjoint $(L_D^{\theta_j})^*:L^2(0,k_{\max})\to L^2(D)$,

$$\left(\left(L_D^{\theta_j}\right)^*\phi\right)(y) := \int_0^{k_{\max}} e^{\mathrm{i}s\theta_j\cdot y}\phi(s)\,\mathrm{d}s\,, \qquad y\in D\,. \tag{3.3}$$

We have the following factorization theorem for F^{θ_j}.

Theorem 3.1. *Let $F^{\theta_j}:L^2(0,k_{\max})\to L^2(0,k_{\max})$ be defined by (3.1). Then*

$$F^{\theta_j} = L_D^{\theta_j}T_D\left(L_D^{\theta_j}\right)^*$$

with $L_D^{\theta_j}$ and $(L_D^{\theta_j})^*$ from (3.2) and (3.3), respectively. The operator $T_D:L^2(D)\to L^2(D)$ is a multiplication operator given by $T_Dg=fg$, where as before $f\in L^\infty(D)$ denotes the source radiating the far field u^∞ as in (2.3).

Proof. Let $\phi\in L^2(0,k_{\max})$. Then, for any $t\in(0,k_{\max})$,

$$\begin{aligned}
\left(L_D^{\theta_j}T_D\left(L_D^{\theta_j}\right)^*\phi\right)(t) &= \int_D e^{-\mathrm{i}t\theta_j\cdot y}\left(T_D\left(L_D^{\theta_j}\right)^*\phi\right)(y)\,\mathrm{d}y\\
&= \int_D e^{-\mathrm{i}t\theta_j\cdot y}f(y)\int_0^{k_{\max}}\phi(s)e^{\mathrm{i}s\theta_j\cdot y}\,\mathrm{d}s\,\mathrm{d}y\\
&= \int_0^{k_{\max}}\phi(s)\int_D e^{-\mathrm{i}(t-s)\theta_j\cdot y}f(y)\,\mathrm{d}y\,\mathrm{d}s = \int_0^{k_{\max}}\phi(s)u^\infty(\theta_j;t-s)\,\mathrm{d}s\\
&= \left(F^{\theta_j}\phi\right)(t)\,.
\end{aligned}$$

∎

Next we establish a density result for $L_D^{\theta_j}$.

Lemma 3.2. *The operator $L_D^{\theta_j}$ is compact with dense range.*

Proof. Let $\phi \in L^2(0, k_{\max})$ and denote by $\widetilde{\phi} \in L^2(\mathbb{R})$ the extension of ϕ to $\mathbb{R}$ that is zero outside $(0, k_{\max})$. Then

$$\left(\left(L_D^{\theta_j}\right)^* \phi\right)(y) = \int_0^{k_{\max}} e^{\mathrm{i}s\theta_j \cdot y} \phi(s)\, \mathrm{d}s = \int_{-\infty}^{\infty} e^{\mathrm{i}s\theta_j \cdot y} \widetilde{\phi}(s)\, \mathrm{d}s\,, \qquad y \in D\,,$$

coincides (up to a constant factor) with the inverse Fourier transform of $\widetilde{\phi}$ on the open subset $\theta_j \cdot D \subseteq \mathbb{R}$. The latter is analytic, because $\widetilde{\phi}$ is compactly supported. Therefore, if $(L_D^{\theta_j})^* \phi = 0$ on D, then $\widetilde{\phi} = 0$ on $\mathbb{R}$ by analytic continuation, and thus $\phi = 0$ on $(0, k_{\max})$. Hence, $(L_D^{\theta_j})^*$ is one-to-one, and since $\overline{\mathcal{R}(L_D^{\theta_j})} = \mathcal{N}((L_D^{\theta_j})^*)^\perp$, this shows that $L_D^{\theta_j}$ has dense range.

The compactness of $L_D^{\theta_j}$ follows immediately from (3.2). ∎

We have the following lemma describing the dependence of the range of the operator $L_D^{\theta_j}$ on the projection $(\theta_j \cdot D)\theta_j$ of the domain D on the one-dimensional subspace of $\mathbb{R}^d$ that is spanned by the observation directions $\pm\theta_j$.

Lemma 3.3. *Let $\Omega_1, \Omega_2 \subseteq \mathbb{R}^d$ be bounded domains, and let $L_{\Omega_\ell}^{\theta_j} : L^2(\Omega_\ell) \to L^2(0, k_{\max})$, $\ell = 1, 2$, be defined as in (3.2) (with D replaced by Ω_ℓ). If $\theta_j \cdot \Omega_1 \cap \theta_j \cdot \Omega_2 = \emptyset$, then the ranges of $L_{\Omega_1}^{\theta_j}$ and $L_{\Omega_2}^{\theta_j}$ have trivial intersection, i.e., $\mathcal{R}(L_{\Omega_1}^{\theta_j}) \cap \mathcal{R}(L_{\Omega_2}^{\theta_j}) = \{0\}$.*

Proof. Suppose that $\theta_j \cdot \Omega_1 \cap \theta_j \cdot \Omega_2 = \emptyset$. Applying the Fourier slice theorem as in (2.8) we find that for any $\psi_\ell \in L^2(\Omega_\ell)$, $\ell = 1, 2$,

$$\left(L_{\Omega_\ell}^{\theta_j} \psi_\ell\right)(t) = \widehat{\psi}_\ell(t\theta_j) = \left(\widehat{R_{\Omega_\ell}^{\theta_j} \psi_\ell}\right)(t)\,, \qquad t \in (0, k_{\max})\,,$$

where $R_{\Omega_\ell}^{\theta_j} : L^2(\Omega_\ell) \to L^1(\mathbb{R})$,

$$\left(R_{\Omega_\ell}^{\theta_j} \psi_\ell\right)(s) := \int_{\theta_j^\perp} \psi_\ell(s\theta_j + y)\, \mathrm{d}y\,, \qquad s \in \mathbb{R}\,, \tag{3.4}$$

denotes the (bounded extension of the) Radon transform in the hyperplane perpendicular to θ_j. Accordingly, it suffices to show that

$$\mathcal{R}\left(R_{\Omega_1}^{\theta_j}\right) \cap \mathcal{R}\left(R_{\Omega_2}^{\theta_j}\right) = \{0\}\,.$$

However, since $\overline{\theta_j \cdot \Omega_1} \cap \overline{\theta_j \cdot \Omega_2}$ has measure zero, the latter follows immediately from the fact that, for $\ell = 1, 2$,

$$\operatorname{supp}\left(R_{\Omega_\ell}^{\theta_j} \psi_\ell\right) \subseteq \overline{\theta_j \cdot \Omega_\ell} \qquad \text{for all } \psi_\ell \in L^2(\Omega_\ell)\,.$$ ∎

The next step in the derivation of the factorization method for one fixed pair of observation directions $\pm\theta_j$ is a characterization of the projection $(\theta_j \cdot D)\theta_j$ of D on the one-dimensional subspace of $\mathbb{R}^d$ that is spanned by $\pm\theta_j$ in terms of the range of the operator $L_D^{\theta_j}$.

Lemma 3.4. *For any $z \in \mathbb{R}^d$ and $\varepsilon > 0$ let the* test function $\phi_{z,\varepsilon}^{\theta_j} \in L^2(0, k_{\max})$ *be defined by*

$$\phi_{z,\varepsilon}^{\theta_j}(t) := \frac{1}{|B_\varepsilon(z)|} \int_{B_\varepsilon(z)} e^{-\mathrm{i}t\theta_j \cdot y} \, \mathrm{d}y \,, \qquad t \in (0, k_{\max}) \,, \tag{3.5}$$

where $B_\varepsilon(z)$ denotes the ball of radius ε centered at z and $|B_\varepsilon(z)|$ its volume.

(a) *If $\theta_j \cdot z \in \theta_j \cdot D$, then there exists $\varepsilon > 0$ such that $\phi_{z,\varepsilon}^{\theta_j} \in \mathcal{R}(L_D^{\theta_j})$.*

(b) *For any $\varepsilon > 0$,*

$$\theta_j \cdot B_\varepsilon(z) \cap \theta_j \cdot D = \emptyset$$

implies that $\phi_{z,\varepsilon}^{\theta_j} \notin \mathcal{R}(L_D^{\theta_j})$.

Proof.

(a) If $\theta_j \cdot z \in \theta_j \cdot D$, then there exists $y \in D$ such that $\theta_j \cdot z = \theta_j \cdot y$, and since $D \subseteq \mathbb{R}^d$ is open, there exists $\varepsilon > 0$ such that $B_\varepsilon(y) \subseteq D$. Accordingly, $B_\varepsilon(z) \cdot \theta_j = B_\varepsilon(y) \cdot \theta_j$ and therefore

$$\frac{1}{|B_\varepsilon(y)|} L_D^{\theta_j} \chi_{B_\varepsilon(y)} = \phi_{z,\varepsilon}^{\theta_j} \,,$$

where $\chi_{B_\varepsilon(y)}$ denotes the characteristic function on $B_\varepsilon(y)$. Hence $\phi_{z,\varepsilon}^{\theta_j} \in \mathcal{R}(L_D^{\theta_j})$.

(b) On the other hand, if $\theta_j \cdot B_\varepsilon(z) \cap \theta_j \cdot D = \emptyset$, then Lemma 3.3 shows that

$$\mathcal{R}\left(L_{B_\varepsilon(z)}^{\theta_j}\right) \cap \mathcal{R}\left(L_D^{\theta_j}\right) = \{0\} \,.$$

Since $0 \neq \phi_{z,\varepsilon}^{\theta_j} = \frac{1}{|B_\varepsilon(z)|} L_{B_\varepsilon(z)}^{\theta_j} \chi_{B_\varepsilon(z)} \in \mathcal{R}(L_{B_\varepsilon(z)}^{\theta_j})$, this implies that $\phi_{z,\varepsilon}^{\theta_j} \notin \mathcal{R}(L_D^{\theta_j})$. ∎

Remark 3.5. In particular, Lemma 3.4 shows that for any $\varepsilon > 0$ the condition $\phi_{z,\varepsilon}^{\theta_j} \in \mathcal{R}(L_D^{\theta_j})$ implies that $\theta \cdot B_\varepsilon(z) \cap \theta \cdot D \neq \emptyset$.

Next we express the range of $L_D^{\theta_j}$ in terms of the operator F^{θ_j}.

Theorem 3.6. *Assume that there exists $\tau \in \mathbb{R}$ and a constant $c_0 > 0$ such that $\mathrm{Re}(e^{\mathrm{i}\tau} f(x)) \geq c_0$ for almost every $x \in D$. Then the self-adjoint operator*

$$F_\#^{\theta_j} := \mathrm{Re}(e^{\mathrm{i}\tau} F^{\theta_j}) := \frac{1}{2}(e^{\mathrm{i}\tau} F^{\theta_j} + e^{-\mathrm{i}\tau} (F^{\theta_j})^*) \tag{3.6}$$

is positive and satisfies $\mathcal{R}(L_D^{\theta_j}) = \mathcal{R}((F_\#^{\theta_j})^{1/2})$.

Proof. From Lemma 3.2 we already know that $L_D^{\theta_j}$ is compact with dense range and accordingly its adjoint $(L_D^{\theta_j})^*$ is compact and one-to-one. Furthermore, since $\mathrm{Re}(e^{\mathrm{i}\tau} f(x)) \geq c_0$ by assumption, we find that

$$\mathrm{Re}(e^{\mathrm{i}\tau} \langle Tg, g \rangle_{L^2(D)}) = \int_D \mathrm{Re}(e^{\mathrm{i}\tau} f(x)) |g(x)|^2 \, \mathrm{d}x \geq c_0 \|g\|_{L^2(D)}^2 \,,$$

i.e., the operator $\mathrm{Re}(e^{\mathrm{i}\tau} T)$ is coercive. Therefore, applying Theorem 4.1 in [24] shows that $\mathcal{R}(L_D^{\theta_j}) = \mathcal{R}((F_\#^{\theta_j})^{1/2})$. ∎

Putting Lemma 3.4 and Theorem 3.6 together, and recalling (2.7), we arrive at the following characterization of the support D of the source f in terms of the operator $F_\#^{\theta_j}$, i.e., in terms of the far field data $u^\infty(\pm\theta_j;k)$, $k\in(0,k_{\max})$, measured in the observation directions $\pm\theta_j$. We use $\mathrm{int}(\Omega)$ to denote the set of all interior points of a set $\Omega\subseteq\mathbb{R}^d$.

Theorem 3.7. *Under the assumptions of Theorem 3.6 we have the following for any $z\in\mathbb{R}^d$:*

(a) *If $z\in\bigcup_{m=1}^M \mathrm{int}(K_{s_{D_m}}(\{\pm\theta_j\}))$, then there exists $\varepsilon>0$ such that $\phi_{z,\varepsilon}^{\theta_j}\in\mathcal{R}((F_\#^{\theta_j})^{1/2})$.*

(b) *If $z\notin\bigcup_{m=1}^M K_{s_{D_m}}(\{\pm\theta_j\})$, then there exists $\varepsilon_0>0$ such that $\phi_{z,\varepsilon}^{\theta_j}\notin\mathcal{R}((F_\#^{\theta_j})^{1/2})$ for any $0<\varepsilon\le\varepsilon_0$.*

Here again $F_\#^{\theta_j}=\mathrm{Re}(e^{\mathrm{i}\tau}F^{\theta_j})$ and $\phi_{z,\varepsilon}^{\theta_j}(t)=(1/|B_\varepsilon(z)|)\int_{B_\varepsilon(z)}e^{-\mathrm{i}t\theta_j\cdot y}\,\mathrm{d}y$, $t\in(0,k_{\max})$.

Proof.

(a) If $z\in\bigcup_{m=1}^M \mathrm{int}(K_{s_{D_m}}(\{\pm\theta_j\}))$, then $\theta_j\cdot z\in\theta_j\cdot D$ and Lemma 3.4(a) together with the range identity in Theorem 3.6 shows that there exists $\varepsilon>0$ such that $\phi_{z,\varepsilon}^{\theta_j}\in\mathcal{R}(L_D^{\theta_j})=\mathcal{R}((F_\#^{\theta_j})^{1/2})$.

(b) On the other hand, if $z\notin\bigcup_{m=1}^M K_{s_{D_m}}(\{\pm\theta_j\})$, then $\theta_j\cdot z\notin\overline{\theta_j\cdot D}$ and there exists $\varepsilon_0>0$ such that $\theta_j\cdot B_\varepsilon(z)\cap\theta_j\cdot D=\emptyset$ for any $0<\varepsilon\le\varepsilon_0$. Accordingly, by Lemma 3.4(b) and Theorem 3.6 we obtain that $\phi_{z,\varepsilon}^{\theta_j}\notin\mathcal{R}((F_\#^{\theta_j})^{1/2})$. ∎

4. Numerical implementation for a single observation direction. Theorem 3.7 says that the far field data $u^\infty(\pm\theta_j;k)$, $k\in(0,k_{\max})$, for a single pair of observation directions $\pm\theta_j\in\Theta$ uniquely determine the smallest union of strips perpendicular to $\pm\theta_j$ that contains all sources. This can be translated in a numerical reconstruction scheme as follows. Denoting by $\{(\lambda_n^{\theta_j},\psi_n^{\theta_j})\mid n\in\mathbb{N}\}$ an eigensystem of the positive and self-adjoint operator $F_\#^{\theta_j}$, Picard's theorem (cf., e.g., [6, Thm. 4.8]) shows that for any $\varepsilon>0$

$$\phi_{z,\varepsilon}^{\theta_j}\in\mathcal{R}((F_\#^{\theta_j})^{1/2})\qquad\text{if and only if}\qquad\sum_{n=1}^\infty\frac{|\langle\phi_{z,\varepsilon}^{\theta_j},\psi_n^{\theta_j}\rangle_{L^2(0,k_{\max})}|^2}{\lambda_n^{\theta_j}}<\infty\,.$$

Therefore, defining the *indicator function*

$$W_\varepsilon^{\theta_j}(z):=\left(\sum_{n=1}^\infty\frac{|\langle\phi_{z,\varepsilon}^{\theta_j},\psi_n^{\theta_j}\rangle_{L^2(0,k_{\max})}|^2}{\lambda_n^{\theta_j}}\right)^{-1},\qquad z\in\mathbb{R}^d\,,\tag{4.1}$$

Theorem 3.7 can be rephrased as follows.

Corollary 4.1. *Under the assumptions of Theorem 3.6 we have the following for any $z\in\mathbb{R}^d$:*

(a) *If $z\in\bigcup_{m=1}^M \mathrm{int}(K_{s_{D_m}}(\{\pm\theta_j\}))$, then there exists $\varepsilon>0$ such that $W_\varepsilon^{\theta_j}(z)>0$.*

(b) *If $z\notin\bigcup_{m=1}^M K_{s_{D_m}}(\{\pm\theta_j\})$, then there exists $\varepsilon_0>0$ such that $W_\varepsilon^{\theta_j}(z)=0$ for any $0<\varepsilon\le\varepsilon_0$.*

In our numerical examples below we consider $2N$ equidistant samples $u^\infty(\pm\theta_j;k_n)$, $n=1,\dots,N$, of the far field, where

$$k_n:=\left(n-\frac{1}{2}\right)\Delta k\qquad\text{with}\quad\Delta k:=\frac{k_{\max}}{N}>0\,.\tag{4.2}$$

Recalling (2.5), this data set is equivalent to

$$u^\infty(\theta_j;-k_N),\dots,u^\infty(\theta_j;-k_1),u^\infty(\theta_j;k_1),\dots,u^\infty(\theta_j;k_N)\,. \tag{4.3}$$

To determine an appropriate sampling rate Δk in (4.2), we utilize once more the Fourier slice theorem

$$u^\infty(\theta_j;k) \;=\; \widehat{f}(k\theta) \;=\; \left(\widehat{R_D^{\theta_j} f}\right)(k)\,, \qquad k\in\mathbb{R}\,,$$

where $R_D^{\theta_j}$ is the Radon transform in the hyperplane perpendicular to θ_j as defined in (3.4). Since $\operatorname{supp}(R_D^{\theta_j} f)\subseteq[-R,R]$, where $R>0$ is the radius of the smallest ball centered at the origin that contains the support of the source f, we find that $u^\infty(\theta_j;\cdot)$ is R-band-limited. Accordingly, the Nyquist condition (cf., e.g., [30, sect. III.1]) suggests choosing

$$\Delta k \;\le\; \frac{\pi}{R}\,. \tag{4.4}$$

Using the $2N$ equidistant samples of the far field in (4.3) and applying the midpoint rule we obtain for the convolution operator F^{θ_j} from (3.1) that

$$\left(F^{\theta_j}\phi\right)(t_p) \;=\; \int_0^{k_{\max}} u^\infty(\theta_j;t_p-s)\phi(s)\,\mathrm{d}s \;\approx\; \Delta k\sum_{\ell=1}^{N} u^\infty(\theta_j;t_p-s_\ell)\phi(s_\ell)$$

for $t_p:=p\Delta k$ and $p=0,\dots,N-1$. Here $s_\ell:=(\ell-\frac{1}{2})\Delta k$ for $\ell=1,\dots,N$. Accordingly, a discrete approximation of F^{θ_j} is given by the Toeplitz matrix

$$\boldsymbol{F}^{\theta_j} \;:=\; \Delta k\begin{bmatrix} u^\infty(\theta_j;-k_1) & u^\infty(\theta_j;-k_2) & \cdots & u^\infty(\theta_j;-k_N)\\ u^\infty(\theta_j;k_1) & u^\infty(\theta_j;-k_1) & \cdots & u^\infty(\theta_j;-k_{N-1})\\ \vdots & & & \vdots\\ u^\infty(\theta_j;k_{N-1}) & u^\infty(\theta_j;k_{N-2}) & \cdots & u^\infty(\theta_j;-k_1)\end{bmatrix}\in\mathbb{C}^{N\times N}\,,$$

and accordingly,

$$\boldsymbol{F}_{\#}^{\theta_j} \;:=\; \frac{1}{2}\left(e^{\mathrm{i}\tau}\boldsymbol{F}^{\theta_j}+e^{-\mathrm{i}\tau}(\boldsymbol{F}^{\theta_j})^*\right) \tag{4.5}$$

is a finite dimensional realization of the operator $F_{\#}^{\theta_j}$ from (3.6).

Similarly, we discretize the test function $\phi_{z,\varepsilon}^{\theta_j}$ from (3.5) by the *test vector*

$$\boldsymbol{\phi}_z^{\theta_j} \;:=\; \left[e^{-\mathrm{i}t_0\theta_j\cdot z},\dots,e^{-\mathrm{i}t_{N-1}\theta_j\cdot z}\right]^T\in\mathbb{C}^N\,, \qquad z\in\mathbb{R}^d\,. \tag{4.6}$$

Since we can choose the parameter $\varepsilon>0$ in the reconstruction method arbitrarily small, this is justified by Taylor's theorem.

Remark 4.2. We note that the upper bound on Δk in (4.4) ensures that $|\Delta k(\theta_j\cdot z)|<\pi$ for any $z\in B_R(0)$. In particular no two points in the region of interest $B_R(0)$ share the same test vector $\boldsymbol{\phi}_z^{\theta_j}$.

Denoting by $\{(\widetilde{\lambda}_n^{\theta_j}, \widetilde{\psi}_n^{\theta_j}) \mid n = 1, \dots, N\}$ an eigensystem of the self-adjoint matrix $\boldsymbol{F}_{\#}^{\theta_j}$, we approximate the indicator function $W_\varepsilon^{\theta_j}$ from (4.1) by

$$W_N^{\theta_j}(z) := \left(\sum_{n=1}^{N} \frac{|(\boldsymbol{\phi}_z^{\theta_j})^* \widetilde{\psi}_n^{\theta_j}|^2}{\widetilde{\lambda}_n^{\theta_j}} \right)^{-1}, \qquad z \in B_R(z). \tag{4.7}$$

From Corollary 4.1 we expect that $W_N^{\theta_j}(z)$ is much larger for $z \in \bigcup_{m=1}^M K_{s_{D_m}}(\{\pm\theta_j\})$ than for $z \notin \bigcup_{m=1}^M K_{s_{D_m}}(\{\pm\theta_j\})$. Accordingly, a plot of $W_N^{\theta_j}(z)$, $z \in B_R(0)$, should yield a visualization of the union of strips $\bigcup_{m=1}^M K_{s_{D_m}}(\{\pm\theta_j\})$.

Choosing a suitable threshold parameter $\delta > 0$, this suggests that the *numerical range criterion*

$$z \in \bigcup_{m=1}^{M} \widetilde{K}_{s_{D_m}}(\{\pm\theta_j\}) \quad \text{if and only if} \quad W_N^{\theta_j}(z) > \delta \tag{4.8}$$

for any $z \in B_R(0)$ determines an approximation $\bigcup_{m=1}^M \widetilde{K}_{s_{D_m}}(\{\pm\theta_j\})$ of $\bigcup_{m=1}^M K_{s_{D_m}}(\{\pm\theta_j\})$ in the region of interest $B_R(0)$.

Example 4.3. We illustrate the reconstruction procedure for a single pair of observation directions by a two-dimensional numerical example. Let $f = f_1 + f_2$ be a superposition of two compactly supported sources,

$$f_1(x) := \mathrm{i}(1.1 + \sin(x_1)), \qquad x = (x_1, x_2) \in D_1,$$
$$f_2(x) := 3(2 + \cos(x_2)), \qquad x = (x_1, x_2) \in D_2,$$

where D_1 is an ellipsoidal domain and D_2 is a kite-shaped domain as shown in Figure 2 (left). This source satisfies the coercivity assumption from Theorem 3.6 with $\tau = -\pi/4$. We note that the strength of the ellipsoidal source component is considerably lower than that of the kite-shaped source component, and therefore the ellipsoidal source can hardly be distinguished

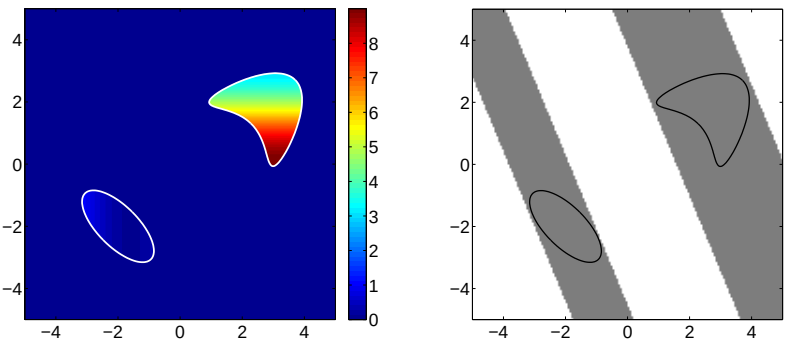

Figure 2. *Left: Absolute values of the source f (color coded), support of the source (solid line). Right: Reconstruction $\{W_{16}^{\theta_j} > 2.5 \cdot 10^{-3}\}$ for a single pair of observation direction $\pm\theta_j$ (gray), support of the source (solid line).*

from the background in this plot. The support of f is contained in the ball of radius $R = 6$ centered at the origin. We consider simulated far field data $u^\infty(\pm\theta_j; k_n)$ radiated by f for a single pair of observation directions $\pm\theta_j = \pm(\cos(\pi/8), \sin(\pi/8)) \in S^1$ at $N = 16$ different wave numbers $k_n = (n-1/2)\Delta k$, $n = 1, \dots, N$. Here we use $\Delta k = \pi/6 \approx 0.52$, as suggested in (4.4), i.e., the smallest and largest wave numbers are $k_{\min} \approx 0.26$ and $k_{\max} \approx 8.12$, respectively.

We compute the eigenvalues and eigenvectors of the matrix $\boldsymbol{F}_{\#}^{\theta_j} \in \mathbb{C}^{16\times 16}$ from (4.5) (using the parameter $\tau = -\pi/4$, which we assume to be known) and evaluate the indicator function $W_{16}^{\theta_j}$ from (4.7) on the square $[-5, 5]^2$. Applying the numerical range criterion (4.8) with threshold parameter $\delta = 2.5 \cdot 10^{-3}$, we show in Figure 2 (right) a visualization of the reconstruction

$$\{x \in [-5, 5]^2 \mid W_{16}^{\theta_j}(x) > \delta\}$$

(gray ribbons). For comparison we have also included the boundary of the support of the source f in this plot (solid line). As predicted by our theoretical results, the reconstruction nicely approximates the smallest union of strips perpendicular to the observation directions $\pm\theta_j$ that contains the source, i.e., $K_{s_{D_1}}(\{\pm\theta_j\}) \cup K_{s_{D_2}}(\{\pm\theta_j\})$.

To illustrate the sensitivity of this reconstruction with respect to the threshold parameter δ, we include in Figure 3 (left) a semilogarithmic plot of a cross section $W_{16}^{\theta_j}(s\theta_j)$, $-5 \le s \le 5$, parallel to $\pm\theta_j$. The dashed line corresponds to the threshold parameter $\delta = 2.5 \cdot 10^{-3}$ used in this example. The indicator function decays rapidly away from $K_{s_{D_1}}(\{\pm\theta_j\}) \cup K_{s_{D_2}}(\{\pm\theta_j\})$, which indicates that useful reconstructions are obtained for an acceptably wide range of values for δ.

Getting back to our discussion in Remark 2.2(b) we show in Figure 3 (right) an approximation of the absolute value of the Radon transform $|(Rf)(\theta_j, \cdot)|$ obtained by a discrete inverse Fourier transform of the data $u^\infty(\pm\theta_j; k_n)$, $1 \le n \le N$. Since these data are band-limited, this reconstruction is blurred and shows the typical oscillatory behavior. It is arguably much easier to estimate the support of the source in direction $\pm\theta_j$ from the plot on the left-hand side of Figure 3 than from the plot on the right-hand side.

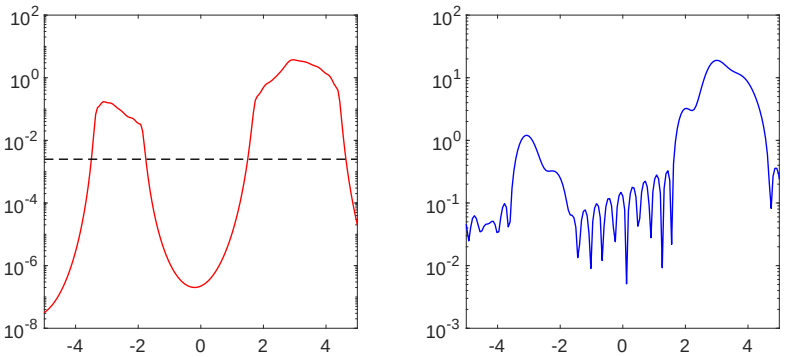

Figure 3. *Left: Cross section of $W_{16}^{\theta_j}$ parallel to the observation directions $\pm\theta_j$ (solid line), threshold $\delta = 2.5 \cdot 10^{-3}$ (dashed line). Right: Cross section of an approximation of $|(Rf)(\theta_j, \cdot)|$ parallel to the observation directions $\pm\theta_j$ obtained from the data.*

5. The reconstruction scheme for multiple observation directions. Next we discuss an extension of the reconstruction method developed in sections 3–4 to multiple observation directions $\pm\theta_1, \dots, \pm\theta_J \in \Theta$, i.e., to the data set given in (2.6). We introduce the generalized indicator function

$$W_\varepsilon^\Theta(z) := \left(\sum_{j=1}^{J} \sum_{n=1}^{\infty} \frac{|\langle \phi_{z,\varepsilon}^{\theta_j}, \psi_n^{\theta_j} \rangle_{L^2(0,k_{\max})}|^2}{\lambda_n^{\theta_j}} \right)^{-1}, \qquad z \in \mathbb{R}^d,$$

where as before, for each pair of observation directions $\pm\theta_j$, the test function $\phi_{z,\varepsilon}^{\theta_j}$ is given by (3.5), and $\{(\lambda_n^{\theta_j}, \psi_n^{\theta_j}) \mid n \in \mathbb{N}\}$ denotes an eigensystem of the operator $F_\#^{\theta_j}$ in (3.6).

Combining the characterization of the support of the source from Theorem 3.7 and Corollary 4.1 for all available pairs of receiver directions $\pm\theta_1, \dots, \pm\theta_J \in \Theta$ we obtain the following result.

Corollary 5.1. *Under the assumptions of Theorem 3.6 we have the following for any $z \in \mathbb{R}^d$:*

(a) *If $z \in \bigcap_{j=1}^J \bigcup_{m=1}^M \operatorname{int}(K_{s_{D_m}}(\{\pm\theta_j\}))$, then there exists $\varepsilon > 0$ such that $\phi_{z,\varepsilon}^{\theta_j} \in \mathcal{R}((F_\#^{\theta_j})^{1/2})$ for any $1 \le j \le J$, or equivalently $W_\varepsilon^\Theta(z) > 0$.*

(b) *If $z \notin \bigcap_{j=1}^J \bigcup_{m=1}^M K_{s_{D_m}}(\{\pm\theta_j\})$, then there exists $1 \le j \le J$ and $\varepsilon_0 > 0$ such that $\phi_{z,\varepsilon}^{\theta_j} \notin \mathcal{R}((F_\#^{\theta_j})^{1/2})$ for any $0 < \varepsilon \le \varepsilon_0$, or equivalently $W_\varepsilon^\Theta(z) = 0$ for any $0 < \varepsilon \le \varepsilon_0$.*

Since

$$\bigcup_{m=1}^{M} K_{s_{D_m}}(\Theta) \subseteq \bigcap_{j=1}^{J} \bigcup_{m=1}^{M} K_{s_{D_m}}(\{\pm\theta_j\}) \subseteq K_{s_D}(\Theta),$$

Corollary 5.1 gives a rigorous characterization of a subset of the Θ-convex hull of the support D of the source, which contains the Θ-convex hull of the support D_m, $m = 1, \dots, M$, of each individual source component, in terms of the measured data (2.6).

The numerical implementation of Corollary 5.1 proceeds along the lines of section 4. For each pair of observation directions $\pm\theta_j$, $j = 1, \dots, J$, we compute the corresponding eigenvectors and eigenvalues $\{(\widetilde{\lambda}_n^{\theta_j}, \widetilde{\psi}_n^{\theta_j}) \mid n = 1, \dots, N\}$ of the matrix $\boldsymbol{F}_\#^{\theta_j}$ and evaluate the approximate indicator function

$$W_N^\Theta(z) := \sum_{j=1}^{J} \left(\sum_{n=1}^{N} \frac{|(\boldsymbol{\phi}_z^{\theta_j})^* \widetilde{\psi}_n^{\theta_j}|^2}{\widetilde{\lambda}_n^{\theta_j}} \right)^{-1}, \qquad z \in B_R(0).$$

Again we expect that the value of $W_N^\Theta(z)$ is much larger for $z \in \bigcap_{j=1}^J \bigcup_{m=1}^M K_{s_{D_m}}(\{\pm\theta_j\})$ than for $z \notin \bigcap_{j=1}^J \bigcup_{m=1}^M K_{s_{D_m}}(\{\pm\theta_j\})$, and plotting $W_N^\Theta(z)$ should yield a visualization of $\bigcap_{j=1}^J \bigcup_{m=1}^M K_{s_{D_m}}(\{\pm\theta_j\})$. Accordingly, choosing a suitable threshold parameter $\delta > 0$, this suggests the *numerical range criterion*

$$z \in \bigcap_{j=1}^{J} \bigcup_{m=1}^{M} \widetilde{K}_{s_{D_m}}(\{\pm\theta_j\}) \quad \text{if and only if} \quad W_N^\Theta(z) > \delta \tag{5.1}$$

for any $z \in B_R(0)$ for determining an approximation $\bigcap_{j=1}^{J} \bigcup_{m=1}^{M} \widetilde{K}_{s_{D_m}}(\{\pm\theta_j\})$ of the set $\bigcap_{j=1}^{J} \bigcup_{m=1}^{M} K_{s_{D_m}}(\{\pm\theta_j\})$ in the region of interest $B_R(0)$.

Example 5.2. We continue Example 4.3, but now we consider $J = 8$ pairs of observation directions

$$\pm\theta_j = \pm\left(\cos\frac{(j-1)\pi}{J}, \sin\frac{(j-1)\pi}{J}\right), \qquad j = 1, \dots, J,$$

and (as before) $N = 16$ different wave numbers $k_n = (n - 1/2)\Delta k$, $n = 1, \dots, N$, with $\Delta k = \pi/6 \approx 0.52$ for each direction.

Applying the numerical range criterion (5.1) with threshold parameter $\delta = 2.5 \cdot 10^{-3}$, we show in Figure 4 (left) a visualization of the reconstruction

$$\{x \in [-5, 5]^2 \mid W_{16}^{\Theta}(x) > \delta\} \tag{5.2}$$

(gray). For comparison we also included the boundary of the support of the source f in this plot (solid line). The reconstruction is very close to the union $\bigcup_{m=1}^{M} K_{s_{D_m}}(\Theta)$ of the Θ-convex hulls of the supports D_m, $m = 1, \dots, M$, of the individual source components.

To get an idea about the sensitivity of the algorithm with respect to noise in the data, we redo this computation but add uniformly distributed relative error to the simulated forward data before starting the reconstruction procedure. The resulting reconstructions are shown in Figure 4 for two different noise levels. In these reconstructions the noise is only accounted for via the threshold parameter δ of (5.2): We use $\delta = 0.01$ for 1% noise and $\delta = 0.02$ for 5% noise. The results clearly get worse with increasing noise level, but they still contain useful information on the location of the sources.

Of course the number of observation directions and the number of frequencies affect the quality of the reconstructions as well: The more data we use, the better are the reconstructions. However, even in the limit as the number of observation directions tends to infinity we cannot expect to recover the exact convex hulls of the supports of the individual source components (cf. Remarks 2.1 and 5.3).

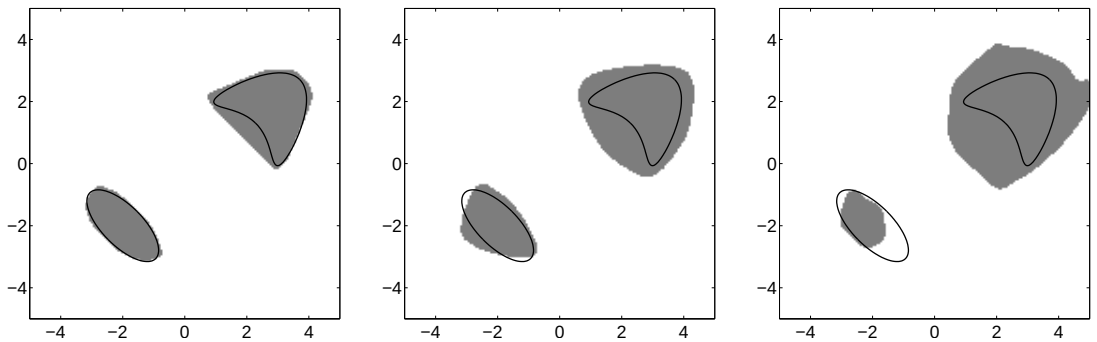

Figure 4. *Reconstructions from* 8 *pairs of observation directions using* 16 *different frequencies each. Left:* 0% *noise. Middle:* 1% *noise. Right:* 5% *noise.*

Remark 5.3. Corollary 5.1 shows that the reconstruction obtained by the algorithm for multiple observation directions based on the numerical range criterion (4.8) approximates the union of convex polygons

$$X := \bigcap_{j=1}^{J} \bigcup_{m=1}^{M} K_{s_{D_m}}(\{\pm\theta_j\}),$$

which is a subset of the Θ-convex hull of the support D of the source that contains the Θ-convex hulls of the supports D_m, $m = 1, \dots, M$, of the individual source components. In case of a single source component these two sets coincide of course. However, if there are two or more well-separated source components, then the reconstruction X might actually be larger than the union of the Θ-convex hulls of the supports of the individual source components, depending on the geometrical configuration.

A glance at the proofs in section 3 reveals that for any $z \in K_{s_D}(\Theta) \setminus \bigcup_{m=1}^{M} K_{s_{D_m}}(\Theta)$ we have that $z \notin X$ (i.e., z is not part of the reconstruction) if and only if there is a pair of observation directions $\pm\theta_j$, $1 \le j \le J$, such that $\theta_j \cdot z \notin \overline{\theta_j \cdot D}$. The latter is equivalent to the condition $(z + \theta_j^{\perp}) \cap \overline{D} = \emptyset$, where $\theta_j^{\perp}$ denotes the hyperplane perpendicular to $\pm\theta_j$. This means that if there is no affine hyperplane perpendicular to a pair of observation directions $\pm\theta_j \in \Theta$ that contains z but does not intersect the support D of the source, then z cannot be identified as a point outside $\bigcup_{m=1}^{M} K_{s_{D_m}}(\Theta)$ by the reconstruction scheme and will be part of the reconstruction. This is more likely to happen if the individual source components are very close to each other relative to their dimensions. For points z outside the Θ-convex hull of the support of the whole collection of sources such an affine hyperplane always exists of course, and therefore the reconstruction X is contained in $K_{s_D}(\Theta)$.

On the positive side we mention that as the size of the supports of the individual source components becomes smaller with respect to their relative distances, the reconstructions get closer to $\bigcup_{m=1}^{M} K_{s_{D_m}}(\Theta)$. In fact we have recently considered the limiting case when the diameters of the supports of the individual source components tend to zero in [15], and we established upper bounds on the number of observation directions and wave numbers that are sufficient to uniquely recover the positions of a finite collection of (infinitesimally small) point sources using a finite dimensional variant of the factorization method presented in this work—a MUSIC algorithm.

6. Possible extensions.

We discuss two possible extensions of the algorithm presented so far. The first concerns the Born approximation of scattering from an inhomogeneous medium, while the second deals with frequency bands bounded away from zero.

6.1. Linearized inverse medium scattering.

Let $D = \bigcup_{m=1}^{M} D_m$ be a collection of well-separated bounded domains, and assume that each subdomain D_m, $m = 1, \dots, M$, represents a scattering object specified by its *refractive index* $n_m^2 = 1 + q_m$ for some $q_m \in L^\infty(D_m)$ with

$$\text{(6.1)} \qquad \operatorname{Re}(q_m) \ge 0, \quad \operatorname{Im}(q_m) \ge 0, \quad \text{and} \quad |q_m| \ge \sqrt{2}c_0 > 0 \quad \text{on } D_m.$$

Suppose that the scatterers are embedded in a homogeneous background medium such that the refractive index n^2 of the whole configuration is given by

$$n^2 \;=\; 1+q \;=\; \begin{cases} n_m^2 & \text{in } D_m\,,\ m=1,\dots,M\,,\\ 1 & \text{in } \mathbb{R}^d \setminus D\,. \end{cases}$$

Denoting by $u^i(\,\cdot\,,\theta;k)$ a time-harmonic plane wave *incident field* with *incident direction* $\theta \in S^{d-1}$ and wave number $k>0$, i.e.,

$$u^i(x,\theta;k) \;=\; e^{\mathrm{i}kx\cdot\theta}\,, \qquad x\in\mathbb{R}^d\,,$$

the mathematical model for scattering by an inhomogeneous medium that we use is the Helmholtz equation

$$\Delta u + k^2 n^2 u \;=\; 0 \qquad \text{in } \mathbb{R}^d\,.$$

We express the total field u in the form $u=u^i+u^s$, where the *scattered field* u^s satisfies the Sommerfeld radiation condition (2.2). Accordingly,

$$-\Delta u - k^2 u \;=\; k^2 q(u^i+u^s) \qquad \text{in } \mathbb{R}^d\,,$$

and the *Born approximation* u_B^s to u^s is the unique solution to

$$-\Delta u_B^s - k^2 u_B^s \;=\; k^2 q u^i \qquad \text{in } \mathbb{R}^d$$

that satisfies the Sommerfeld radiation condition (2.2) (see, e.g., [6, p. 277]). This resembles (2.1)–(2.2) with the source term $f(x)=k^2q(x)e^{\mathrm{i}kx\cdot\theta}$. The Born far field $u_B^\infty(\,\cdot\,,\theta;k)$ of $u_B^s(\,\cdot\,,\theta;k)$ is given by

$$u_B^\infty(\theta_x,\theta;k) \;=\; k^2\int_D e^{-\mathrm{i}k(\theta_x-\theta)\cdot y} q(y)\,\mathrm{d}y \;=\; k^2\widehat{q}(k(\theta_x-\theta))\,, \qquad \theta_x\in S^{d-1}\,,$$

and as before, we extend the definition of u_B^∞ to negative wave numbers by means of

$$u_B^\infty(\theta_x,\theta;-k) \;:=\; u_B^\infty(\theta,\theta_x;k), \qquad \theta_x,\theta\in S^{d-1}\,,\ k>0\,. \tag{6.2}$$

If the observed scattering data allow for a symmetric extension to negative wave numbers as in (6.2), then we can proceed as in sections 3–5 to generalize the reconstruction method to the linearized inverse medium scattering problem. This symmetry condition is, for instance, fulfilled for

(a) symmetric backscattering data, i.e., when far field observations

$$u^\infty(-\theta_j,\theta_j;k) \quad\text{and}\quad u^\infty(\theta_j,-\theta_j;k)\,, \qquad j=1,\dots,J\,,$$

are available for some $\theta_1,\dots,\theta_J \in S^{d-1}$ and for a whole band of wave numbers $k\in(0,k_{\max})$;

(b) symmetric two-point measurements, i.e., when far field observations

$$u^\infty(\theta_{j_1},\theta_{j_2};k) \quad\text{and}\quad u^\infty(\theta_{j_2},\theta_{j_1};k)\,, \qquad j_1,j_2=1,\dots,J\,,\ j_1\neq j_2\,,$$

are available for some $\theta_1,\dots,\theta_J \in S^{d-1}$ and for a whole band of wave numbers $k\in(0,k_{\max})$.

For example, in case of backscattering data we just have to replace the convolution operator in (3.1) for any pair of observation directions $\pm\theta_j$ by $F^{\theta_j} : L^2(0,k_{\max}) \to L^2(0,k_{\max})$,

$$\left(F^{\theta_j}\phi\right)(t) := \int_0^{k_{\max}} \frac{1}{(t-s)^2} u_B^\infty(\theta_j,-\theta_j;t-s)\phi(s)\,\mathrm{d}s\,, \qquad t\in(0,k_{\max})\,.$$

Then, $F^{\theta_j} = L_D^{\theta_j} T_D (L_D^{\theta_j})^*$ with $L_D^{\theta_j} : L^2(D) \to L^2(0,k_{\max})$,

$$\left(L_D^{\theta_j}\psi\right)(t) := \int_D e^{-2\mathrm{i}t\theta_j\cdot y}\psi(y)\,\mathrm{d}y\,, \qquad t\in(0,k_{\max})\,,$$

and the multiplication operator $T_D : L^2(D) \to L^2(D)$, $T_D g = qg$. Our assumptions (6.1) on the contrasts $q_1,\dots,q_M$ imply that

$$\mathrm{Re}\left(e^{-\mathrm{i}\frac{\pi}{4}}q(x)\right) = \frac{1}{\sqrt{2}}(\mathrm{Re}(q(x))+\mathrm{Im}(q(x)) \geq \frac{1}{\sqrt{2}}|q(x)| \geq c_0\,, \qquad x\in D\,,$$

i.e., a coercivity assumption as in Theorem 3.6 is satisfied with $\tau = -\pi/4$. Therewith, the results from sections 3–5 carry over. We only have to replace the test function in (3.5) by $\phi_{z,\varepsilon}^{\theta_j}(t) = (1/|B_\varepsilon(z)|)\int_{B_\varepsilon(z)} e^{-2\mathrm{i}t\theta_j\cdot y}\,\mathrm{d}y$, $t\in(0,k_{\max})$, the test vector in (4.6) by

$$\boldsymbol{\phi}_z^{\theta_j} := \left[e^{-2\mathrm{i}t_0\theta_j\cdot z},\dots,e^{-2\mathrm{i}t_{N-1}\theta_j\cdot z}\right]^T \in \mathbb{C}^N\,, \qquad z\in\mathbb{R}^d\,,$$

and the sampling condition condition (4.4) by $\Delta k \leq \pi/(2R)$.

In case of symmetric two-point measurements we can proceed similarly.

6.2. Frequency bands bounded away from zero. We return to the inverse source problem from section 2, but now we assume that the far field data $u^\infty(\theta;k)$ are given for J observation directions $\theta\in\{\theta_1,\dots,\theta_J\}\in S^{d-1}$ and across a band of wave numbers $k\in(k_{\min},k_{\max})$ for some $k_{\max} > k_{\min} > 0$. In contrast to section 2 the interval of frequencies is bounded away from zero, and the (discrete) set of observation directions is no longer required to be symmetric.

Proceeding as in sections 3–4 the reconstruction method can be generalized to this setting as follows. We denote by $k_c := (k_{\max}+k_{\min})/2$ and $b_k := (k_{\max}-k_{\min})/2$ the *central frequency* and half of the bandwidth of the given far field data.

Replacing the convolution operator in (3.1) for any observation direction θ_j by the operator $F^{\theta_j} : L^2(0,b_k) \to L^2(0,b_k)$,

$$\left(F^{\theta_j}\phi\right)(t) := \int_0^{b_k} u^\infty(\theta_j;k_c+t-s)\phi(s)\,\mathrm{d}s\,, \qquad t\in(0,b_k)\,,$$

we obtain the factorization $F^{\theta_j} = L_D^{\theta_j} T_D^{\theta_j} (L_D^{\theta_j})^*$ with $L_D^{\theta_j} : L^2(D) \to L^2(0,b_k)$,

$$\left(L_D^{\theta_j}\psi\right)(t) := \int_D e^{-\mathrm{i}t\theta_j\cdot y}\psi(y)\,\mathrm{d}y\,, \qquad t\in(0,b_k)\,,$$

and the multiplication operator $T_D^{\theta_j} : L^2(D) \to L^2(D)$,

$$\left(T_D^{\theta_j} g\right)(x) = e^{-\mathrm{i}k_c\theta_j\cdot x} f(x)g(x)\,, \qquad x \in D\,,$$

which now also depends on the observation direction θ_j.

If there exist $\tau \in \mathbb{R}$ and a constant $c_0 > 0$ such that

$$\mathrm{Re}\left(e^{\mathrm{i}\tau} e^{-\mathrm{i}k_c\theta_j\cdot x} f(x)\right) \geq c_0\,, \qquad x \in D\,, \tag{6.3}$$

then the results from sections 3–5 carry over. The condition (6.3) is, e.g., satisfied with $\tau = -\pi/4$ if

$$\mathrm{Re}(f) \geq 0\,, \quad \mathrm{Im}(f) \geq 0, \quad \text{and} \quad |f| \geq \sqrt{2}c_0 > 0 \qquad \text{on } D$$

and if

$$|k_c R| < \frac{\pi}{4}\,, \tag{6.4}$$

where as before $R > 0$ is the radius of the smallest ball centered at the origin that contains the support of the source f. We note that the condition (6.4), which was not required for the original setup in sections 3–5, restricts the size of the central frequency in terms of the diameter of the support of the source.

7. Summary. We have developed a qualitative reconstruction method that can be used to locate several compactly supported sources within a homogeneous background medium from sparse multifrequency far field measurements, provided that the sources satisfy certain coercivity constraints. The reconstruction method efficiently utilizes the multifrequency information contained in the data, and therefore the number of receiver locations required to obtain useful reconstructions can be reduced significantly.

The coercivity constraints on the source that we require to obtain the range identity in Theorem 3.6 are equivalent to the assumptions on the refractive index known from traditional factorization methods [25] and cannot easily be relaxed.

The reconstruction scheme developed in this work is particularly useful in the low-frequency regime, where Fourier inversion techniques suffer from serious blurring effects due to the missing high-frequency information.

Acknowledgment. We would like to thank John Sylvester for valuable discussions on this material and for his careful reading of a first draft of the manuscript.

REFERENCES

[1] C. Alves, R. Kress, and P. Serranho, *Iterative and range test methods for an inverse source problem for acoustic waves*, Inverse Problems, 25 (2009), 055005.

[2] G. Bao, P. Li, J. Lin, and F. Triki, *Inverse scattering problems with multi-frequencies*, Inverse Problems, 31 (2015), 093001.

[3] G. Bao, S. Lu, W. Rundell, and B. Xu, *A recursive algorithm for multifrequency acoustic inverse source problems*, SIAM J. Numer. Anal., 53 (2015), pp. 1608–1628.

[4] A. Canelas, A. Laurain, and A. A. Novotny, *A new reconstruction method for the inverse source problem from partial boundary measurements*, Inverse Problems, 31 (2015), 075009.

[5] Q. Chen, H. Haddar, A. Lechleiter, and P. Monk, A sampling method for inverse scattering in the time domain, Inverse Problems, 26 (2010), 085001.

[6] D. Colton and R. Kress, *Inverse Acoustic and Electromagnetic Scattering Theory*, 3rd ed., Springer, New York, 2013.
[7] B. Diederichs and A. Iske, *Parameter estimation for bivariate exponential sums*, in Proceedings of the IEEE International Conference Sampling Theory and Applications, Washington, DC, 2015, pp. 493–497.
[8] M. Eller and N. P. Valdivia, *Acoustic source identification using multiple frequency information*, Inverse Problems, 25 (2009), 115005.
[9] A. C. Fannjiang, T. Strohmer, and P. Yan, *Compressed remote sensing of sparse objects*, SIAM J. Imaging Sci., 3 (2010), pp. 595–618.
[10] F. Frühauf, O. Scherzer, and A. Leitao, *Analysis of regularization methods for the solution of ill-posed problems involving discontinuous operators*, SIAM J. Numer. Anal., 43 (2005), pp. 767–786.
[11] R. Griesmaier, *Multi-frequency orthogonality sampling for inverse obstacle scattering problems*, Inverse Problems 27 (2011), 085005.
[12] R. Griesmaier and M. Hanke, *Multifrequency impedance imaging with multiple signal classification*, SIAM J. Imaging Sci., 8 (2015), pp. 939–967.
[13] R. Griesmaier, M. Hanke, and T. Raasch, *Inverse source problems for the Helmholtz equation and the windowed Fourier transfrom*, SIAM J. Sci. Comput., 34 (2012), pp. A1544–A1562.
[14] R. Griesmaier, M. Hanke, and T. Raasch, *Inverse source problems for the Helmholtz equation and the windowed Fourier transform* II, SIAM J. Sci. Comput., 35 (2013), pp. A2188–A2206.
[15] R. Griesmaier and C. Schmiedecke, *A multifrequency MUSIC algorithm for locating small inhomogeneities in inverse scattering*, Inverse Problems, 33 (2017), 035015.
[16] Y. Guo, P. Monk, and D. Colton, *Toward a time domain approach to the linear sampling method*, Inverse Problems, 29 (2013), 095016.
[17] B. B. Guzina, F. Cakoni, and C. Bellis, *On the multi-frequency obstacle reconstruction via the linear sampling method*, Inverse Problems, 26 (2010), 125005.
[18] H. Haddar, A. Lechleiter, and S. Simon, *An improved time domain linear sampling method for Robin and Neumann obstacle*, Appl. Anal., 93 (2014), pp. 369–390.
[19] M. Hanke and W. Rundell, *On rational approximation methods for inverse source problems*, Inverse Probl. Imaging, 5 (2011), pp. 185–202.
[20] F. Hettlich and W. Rundell, *Iterative methods for the reconstruction of an inverse potential problem*, Inverse Problems, 12 (1996), pp. 251–266.
[21] M. Ikehata, *Reconstruction of a source domain from the Cauchy data*, Inverse Problems, 15 (1999), pp. 637–645.
[22] V. Isakov, S. Leung, and J. Qian, *A fast local level set method for inverse gravimetry*, Commun. Comput. Phys., 10 (2011), pp. 1044–1070.
[23] A. Kirsch, *Characterization of the shape of a scattering obstacle using the spectral data of the far field operator*, Inverse Problems, 14 (1998), pp. 1489–1512.
[24] A. Kirsch, *The MUSIC algorithm and the factorization method in inverse scattering theory for inhomogeneous media*, Inverse Problems, 18 (2002), pp. 1025–1040.
[25] A. Kirsch and N. Grinberg, *The Factorization Method for Inverse Problems*, Oxford University Press, Oxford, UK, 2008.
[26] S. Kusiak and J. Sylvester, *The scattering support*, Comm. Pure Appl. Math., 56 (2003), pp. 1525–1548.
[27] W. Liao, *MUSIC for multidimensional spectral estimation: Stability and super-resolution*, IEEE Trans. Signal Process., 63 (2015), pp. 6395–6406.
[28] W. Liao and A. Fannjiang, *MUSIC for single-snapshot spectral estimation: Stability and super-resolution*, Appl. Comput. Harmon. Anal., 40 (2016), pp. 33–67.
[29] D. R. Luke, *Multifrequency inverse obstacle scattering: the point source method and generalized filtered backprojection*, Math. Comput. Simulation, 66 (2004), pp. 297–314.
[30] F. Natterer, *The Mathematics of Computerized Tomography*, Teubner/Wiley, New York, 1986.
[31] R. Potthast, *A study on orthogonality sampling*, Inverse Problems, 26 (2010), 074015.
[32] D. Potts and M. Tasche, *Parameter estimation for multivariate exponential sums*, Electron. Trans. Numer. Anal., 40 (2013), pp. 204–224.

[33] J. Sylvester, *Notions of support for far fields*, Inverse Problems, 22 (2006), pp. 1273–1288.
[34] J. Sylvester and J. Kelly, *A scattering support for broadband sparse far field measurements*, Inverse Problems, 21 (2005), pp. 759–771.
[35] X. Wang, Y. Guo, D. Zhang, and H. Liu, *Fourier method for recovering acoustic sources from multi-frequency far-field data*, Inverse Problems, 33 (2017), 035001.